

THE PROCESSING AND INTERPRETATION
OF LONG WAVELENGTH AEROMAGNETIC
ANOMALIES

A THESIS
PRESENTED TO
THE FACULTY OF GRADUATE STUDIES
UNIVERSITY OF MANITOBA

IN PARTIAL FULFILLMENT
OF THE REQUIREMENTS FOR THE DEGREE
MASTER OF SCIENCE, GEOPHYSICS

BY
ALAN M. TANG

OCTOBER 1980

THE PROCESSING AND INTERPRETATION
OF LONG WAVELENGTH AEROMAGNETIC
ANOMALIES

by

ALAN MO-SUM TANG

A thesis submitted to the Faculty of Graduate Studies of
the University of Manitoba in partial fulfillment of the requirements
of the degree of

MASTER OF SCIENCE

©1980

Permission has been granted to the LIBRARY OF THE UNIVERSITY OF MANITOBA to lend or sell copies of this thesis, to the NATIONAL LIBRARY OF CANADA to microfilm this thesis and to lend or sell copies of the film, and UNIVERSITY MICROFILMS to publish an abstract of this thesis.

The author reserves other publication rights, and neither the thesis nor extensive extracts from it may be printed or otherwise reproduced without the author's written permission.

ABSTRACT

Digital data processing techniques are now available and widely used in the study of aeromagnetic surveys. It allows detailed analysis to be made of the shallow and deep crustal magnetic units and also enables the short and long wavelength anomalies to be separated and evaluated.

The origin and nature of the long wavelength anomalies are believed to be closely associated with the deep crustal magnetization. These deep crustal magnetic units in turn are related to crustal structure seen on surface geologic maps. The processing sequence of aeromagnetic data that yields long wavelength aeromagnetic anomalies is compiled and evaluated in this study. Different digital processing techniques are examined and employed in an attempt to put together an efficient aeromagnetic processing system.

A long wavelength aeromagnetic map portraying deep crustal magnetic anomalies in the project area (60.00 to 61.75 degrees North and 102.00 to 94.75 degrees West) is presented. The derived map shows a definite alignment of various long wavelength aeromagnetic anomalies of different sizes in a Northeast-Southwest and East-West orientation. As an aid to the interpretation of these aeromagnetic

anomalies, a method of "inverse" depth and magnetic intensity determinations is introduced. The automated interpretation method is based on the optimization of the best fit anomaly field generated by a vertical-sided prismatic model. This interpretation procedure has eliminated the use of the tedious method of type-curve fitting and manual calculations.

The long wavelength anomalies show a good correlation with the broad features of deep crustal structure. The regional geology of the surrounding areas is reviewed and a strong relation between the long wavelength anomaly system and a major structural feature is found.

ACKNOWLEDGEMENTS

The writer wishes to express his sincere thanks and gratitude to Dr. D.H. Hall of the Department of Earth Sciences, University of Manitoba, for his supervision and for his invaluable advice and encouragement during the various stages of this project.

Thanks are due to Dr. A.G. Green for his help and advice on various research problems that arose during the period of this study.

The invaluable discussion and assistance provided by Mr. C. Hasselfield during the difficult time in programming and processing in this project is much appreciated.

The author also gratefully acknowledges the receipt of a student Fellowship and Assistantship from the Department of Earth Sciences of the University of Manitoba.

TABLE OF CONTENTS

		<u>Page</u>
ABSTRACT		iii
ACKNOWLEDGEMENTS		v
TABLE OF CONTENTS		vi
LIST OF ILLUSTRATIONS		viii
LIST OF TABLES		xi
 <u>Chapter</u>		
1	INTRODUCTION	1
2	DIGITAL PROCESSING OF AEROMAGNETIC DATA	5
	2.1 Processing Sequence	5
	2.2 Two-Dimensional Frequency Aliasing	8
	2.3 Preconditioning of Data	9
	2.4 The Fast Fourier Transform	11
	2.5 Background Field Analysis	13
3	THE AREA UNDER STUDY	19
	3.1 Regional Setting and General Geology	19
	3.2 Data Acquisition	22
4	TWO-DIMENSIONAL DIGITAL FILTERING	24
	4.1 Basic Principles and Design of of a Two-Dimensional Filter	24
	4.2 Space Domain Filter Operator	26
	4.3 Two-Dimensional Filtering in the Frequency Domain	27
	4.4 Frequency Response of Two- Dimensional Filters	30
	4.5 A Discussion of the Filtered Aeromagnetic Maps	40
5	SPECTRAL STUDIES	48
	5.1 Introduction	48
	5.2 One-Dimensional Power Spectra	49
	5.3 Maximum Entropy Spectral Analysis	55
	5.4 Two-Dimensional Power Spectrum Analysis	63
	5.5 Radial Spectrum and Its Interpretation	64

<u>Chapter</u>		<u>Page</u>
6	INTERPRETATION	75
	6.1 Introduction	75
	6.2 Interpretation of the Long-Wave- length Aeromagnetic Anomalies Using Prismatic Blocks	75
	6.3 Discussion	78
7	CONCLUSIONS	84
	BIBLIOGRAPHY	86
	APPENDIX A	
	Three-Dimensional Plots of the Filtered Maps	89
	APPENDIX B	
	Computer Programs	96
	- HIDE 3D	97
	- FILTER 2D	101
	- RAID	115

LIST OF ILLUSTRATIONS

<u>Figure</u>		<u>Page</u>
2.1.1	Flow Diagram of the Processing Sequence	6
2.5.1	International Geomagnetic Reference Field of the Project Area	16
2.5.2	Three-Dimensional Representation of the Geomagnetic Field: N.W.T. 60-61.75 N, 102-94.75 W	17
2.5.3	Map Area (N.W.T. 60-61.75 N, 102-94.75 W) with I.G.R.F. Removed	18
3.1.1	Location Map of the Project Area	20
4.2.2	Filtered Aeromagnetic Map of the Project Area Using the Space Domain Filter Operator (Cutoff Wavelength: 60 km)	28
4.2.3	Three-Dimensional Plot of the Aeromagnetic Data Using the Space Domain Filter Operator (Cutoff Wavelength: 60 km)	29
4.3.1	Filtered Aeromagnetic Map of the Project Area Using Frequency Domain Technique (Cutoff Wavelength: 30 km)	31
4.3.2	Filtered Aeromagnetic Map of the Project Area Using Frequency Domain Technique (Cutoff Wavelength: 40 km)	32
4.3.3	Filtered Aeromagnetic Map of the Project Area Using Frequency Domain Technique (Cutoff Wavelength: 50 km)	33
4.3.4	Filtered Aeromagnetic Map of the Project Area Using Frequency Domain Technique (Cutoff Wavelength: 60 km)	34
4.3.5	Filtered Aeromagnetic Map of the Project Area Using Frequency Domain Technique (Cutoff Wavelength: 70 km)	35
4.4.1	Response Curve of the Seventeen-Point Numerical Filter in the Space Domain	38

<u>Figure</u>	<u>Page</u>	
4.4.2	Flow Diagram to Outline the Technique Used to Obtain the Frequency Characteristics of the 2-D Frequency Domain Filter	39
4.4.3	Fourier Transform Map with Synthetic Coefficients Equal to Ones (Cutoff Wavelength: 30 km)	41
4.4.4	Inverse Fourier Transform Map of the Synthetic Coefficients	42
4.4.5	Three-Dimensional Representations of the Frequency Response of the Frequency Domain Filter (Cutoff Wavelength: 30 km)	43
4.4.6	Three-Dimensional Representations of the Frequency Response of the Frequency Domain Filter (Cutoff Wavelength: 40 km)	44
4.4.7	Three-Dimensional Representations of the Frequency Response of the Frequency Domain Filter (Cutoff Wavelength: 60 km)	45
5.2.1	One-Dimensional Power Spectrum (along Latitude 61.75 degrees N)	53
5.2.2	One-Dimensional Power Spectrum (smoothing applied) (along Latitude 61.75 degrees N)	54
5.3.1	Maximum Entropy Autopower Spectrum (Along Latitude 61.75 Degrees N) (Filter Coefficient: 20)	58
5.3.2	Maximum Entropy Autopower Spectrum (Along Latitude 61.75 Degrees N) (Filter Coefficient: 40)	59
5.3.3	Maximum Entropy Autopower Spectrum (Along Latitude 61.75 degrees N) (Filter Coefficient: 60)	60
5.3.4	Maximum Entropy Autopower Spectrum (Along Latitude 61.08 Degrees N) (Filter Coefficient: 40)	61
5.3.5	Maximum Entropy Autopower Spectrum (Along Latitude 61.08 Degrees N) (Filter Coefficient: 85)	62

<u>Figure</u>		<u>Page</u>
5.4.1	Two-Dimensional Power Estimate of the Project Area	65
5.4.2	Three-Dimensional Representation of the Power Spectrum Estimate of the Project Area	66
5.4.3	Profile Across the Two-Dimensional Power Spectrum (45 degrees Counterclockwise to +x Axis)	67
5.4.4	Profile Across the Two-Dimensional Power Spectrum (90 Degrees Counterclockwise to +x Axis)	68
5.4.5	Profile Across the Two-Dimensional Power Spectrum (135 Degrees Counterclockwise to +x Axis)	69
5.5.1	Radial Spectrum of the Aeromagnetic Map Under Studied	71
5.5.3	Radial Spectrum of the Aeromagnetic Map Under Studied (Smoothing Applied)	73
6.2.1	Schematic Diagram of the Location of Various Interpretive Blocks of the Project Area	77
6.3.1	Location of the Conductive Body of the General Geology of the Churchill Province After Camfield and Gough (1977)	82

LIST OF TABLES

<u>Table</u>		<u>Page</u>
5.5.2	Log Average Power vs. Frequency of the Radial Spectrum	72
5.5.4	Log Average Power vs. Frequency of the Radial Spectrum (Smoothing Applied)	74
6.2.2	Table of the Results of the Blocks from "INVBLOCK"	79

CHAPTER 1

INTRODUCTION

When the total anomaly system composed of short wavelengths anomalies are filtered out of an aeromagnetic map, there remains a relatively broad-trend, low-amplitude and long wavelength anomaly field. These anomalies are termed long-wavelength aeromagnetic anomalies.

Long-wavelength aeromagnetic anomalies show considerable correlation with broad crustal structure and provide valuable information in the study of magnetic units lying in the upper and lower layers of the earth's crust. The present study is part of a continuing program of detailed deep crustal magnetic investigations in Manitoba with extensions up to the Northwest Territories.

In recent years, there has been a rapid development in the digital processing techniques of geophysical data. This study deals with the digital processing and interpretation of aeromagnetic data located in the Northwest Territories directly north of the Manitoba provincial boundary. An attempt is made in this thesis to develop a more efficient processing sequence for regional magnetic anomalies,

including the design of a two-dimensional filter for the aeromagnetic data in the frequency (or wave-number) domain. This is achieved with the fast Fourier transformation algorithm developed by Cooley and Tukey (1965).

Two-dimensional aeromagnetic data can be converted into the frequency domain by applying the forward Fourier transformation. The procedure of using one-dimensional transform to calculate the two-dimensional transform is used so as to cut down the available storage space and computing time. Pretreatment of data is essential. The presence of undesired spikes and trends were acknowledged and a computer program package was written to carry out every step of the processing sequence including the filtering of high frequency components of the anomaly field in the frequency domain.

McGrath and Hall (1969) developed a seventeen-point numerical filter in the space domain to remove short wavelength anomalies from an aeromagnetic map. Linear filtering in the frequency domain is under investigation here and a comparison of the nature of the two types of filter is done on the aeromagnetic map in this project. Moreover, various attempts have been made to display the frequency response of the frequency domain filter.

A great deal of interest has been laid on the representation of potential field data in the frequency domain. For

this reason, spectral analysis has become a routine and essential technique in the processing of aeromagnetic maps. One dimensional power spectrum analysis was performed on a few profiles running east-west within the area of concern. Two dimensional power spectrum was also displayed on part of the area. The Maximum Entropy Method for the power spectral density estimation as developed by Burg (1967, 1968) is also reviewed in this thesis and it was experimentally investigated on a few profiles across the area to serve as a comparison to the more conventional power spectral estimation via the fast Fourier transform algorithm.

One of the major characteristics of deep crustal magnetic anomalies are their low amplitude. The amplitudes of this type of anomaly are often less than 200 nanotesla. This is because of the vertical magnetic field decreases as the depth of source increases. Hence the core generated background field plays an important role in the interpretation of the long wavelength aeromagnetic anomalies. A computer Fortran program issued by the Institute of Geological Sciences, Hailsham, Sussex was used for computing the background field values of the project area. It is based on a specified model adopted after the International Association of Geomagnetism and Aeronomy (IAGA) Symposium held in October, 1968 and is termed as the International Geomagnetic Reference Field (IGRF).

The question of uniqueness and ambiguity of potential field interpretations have been discussed by Skeels (1947), and by Roy (1962). For a given magnetization distribution, there is always a predictable magnetic field but the inverse is not always unique. A given magnetic anomaly field may be caused by an infinite number of magnetic distributions and no unique solution can be clearly defined. In the present project, a direct interpretation using the BLOCK model-fit by Coles (1973) was first used for the anomaly interpretations. Then, an inverse problem¹ was set up, with the input of the field values and using optimization processes, the configuration of the blocks that were most acceptable both physically and geologically were then determined.

-
1. The computer program "INVBLOCK" to provide an indirect iterative method to solve the inverse problem was originally derived and implemented by Mr. C. Hasselfield, programmer, Geophysics Section, University of Manitoba.

CHAPTER 2

DIGITAL PROCESSING OF AEROMAGNETIC DATA

2.1 Processing Sequence

The long-wavelength aeromagnetic anomaly system can be separated from the local anomalies due to shallow, narrow sources by eliminating the high wave number (short wavelength) components of the aeromagnetic map. This can be done in several ways; for example, by upward continuation of low-level magnetics. Alternatively, based on the difference in the frequency (wave-length) characteristics of the two major anomaly types, direct filtering can be used. The processing sequence used here for the preparation of the long-wavelength aeromagnetic maps was based on the direct wavelength filtering technique.

Figure 2.1.1 is a flow diagram of the processing sequence of the digitized aeromagnetic map. The computer program FILTER 2D in Appendix B is a FORTRAN routine based on this sequence.

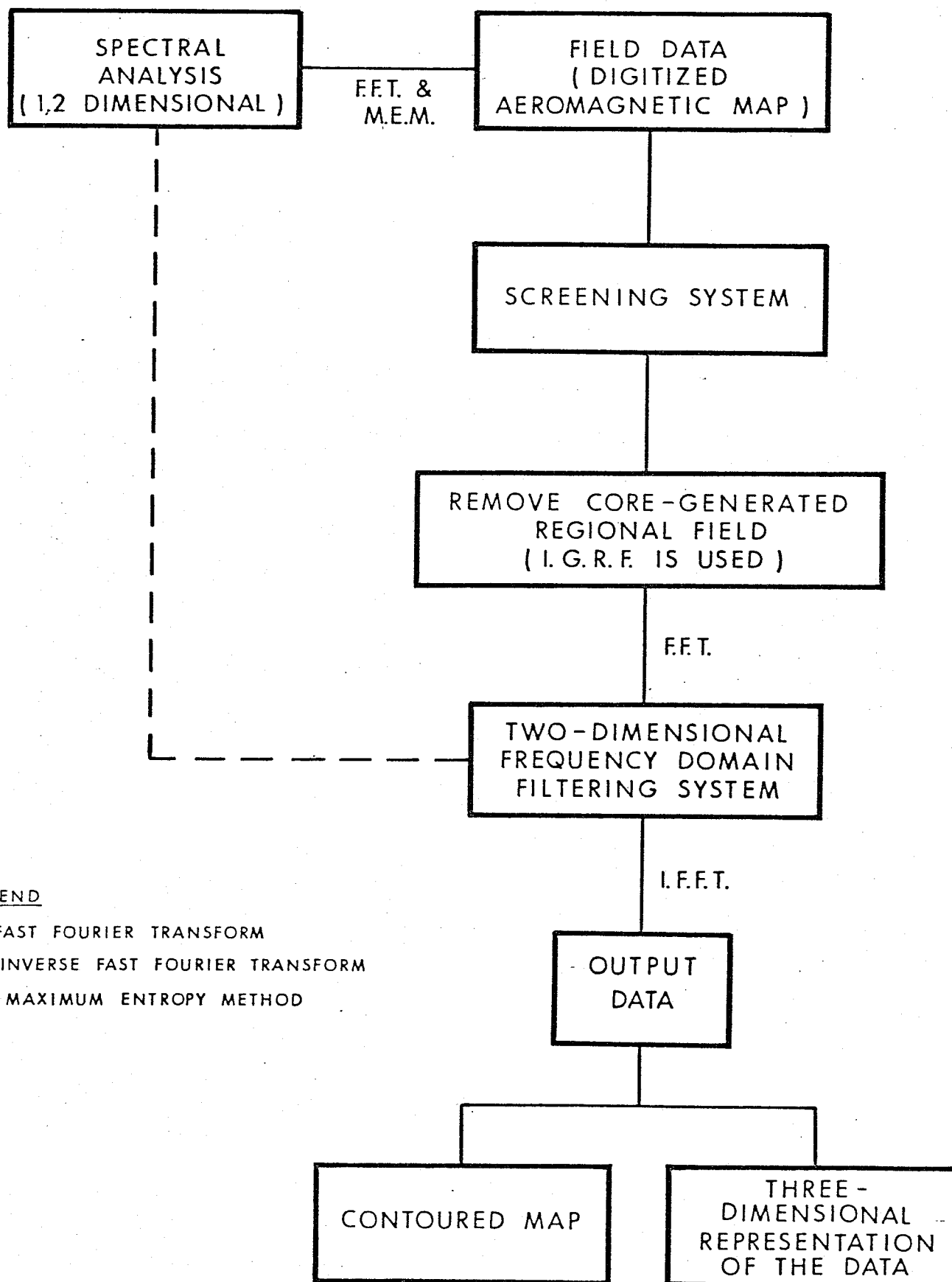


FIGURE 2.1.1. FLOW DIAGRAM OF THE PROCESSING SEQUENCE

It is assumed that the input map consists of digitized data on a regular spaced square or rectangular grid. The sampling (or digital) interval must be equal in the x and y directions.

Both one and two dimensional power spectra were constructed on the data. This analysis provides a spectral scan of the frequency contents of the input map before the filtering technique was applied. Details of the spectral analysis can be found in a later chapter.

Preconditioning of data is also very important. Different screening and smoothing operations were done on the input data before passing the map through the filter system.

After the above steps had been accomplished, the data was then passed into the filter system. Direct filtering in the frequency domain was used in this study. The filter was designed for a series of different cutoff wavelengths and impulse-response of the study map area. To aid interpretation, different displays both in contour map and three-dimensional representation forms were drawn using the IBM calcomp plotter.

2.2 Two-Dimensional Frequency Aliasing

Frequency aliasing is a well-known effect caused by the insufficient sampling of a signal frequency. It occurs when a band limited function is sampled at interval that exceeds $\frac{1}{2f_i}$ where f_i is the highest frequency component of interest recorded.

For two-dimensional data, such as the potential field data, it is necessary to digitize the data from the maps at a suitable sampling interval. A small sampling interval may be desirable since it enables us to study the shorter wavelength anomalies and throw out the aliasing problem. However, one should be aware of the computer limitations in analysing enormous amounts of data and the tedious digitization problem.

Analogous to the one-dimensional case, two-dimensional frequency aliasing rule can be obtained. In order to avoid frequency aliasing when sampling a continuous function band-limited at frequencies of K and L , the sample interval must be selected so that

$$\Delta x \leq \frac{1}{2K} \quad \text{and} \quad \Delta y \leq \frac{1}{2L}$$

In the present project, long-wavelength anomalies with wavelengths usually greater than 60 km are of major concern,

hence, K and L have very high values. The sampling interval of 6.5 km in both x and y directions were selected for the project. This sampling interval was found to be sufficient and reasonable in the computer processing viewpoints and it was done by decimating the unwanted data points in the original data.

2.3 Preconditioning of Data

Preconditioning of data is essential and necessary, especially when filtering in the frequency domain. Spikes appearing in the data, due to digitization error or other data preparation errors, produce problems in the frequency filtering process. It will produce output in the Fourier transform at all frequencies and it must be removed with a search and screening routine. One of the simpler devices for testing doubtful observations is known as "Chauvenet's Criterion of Rejection", according to which rejectability is determined as a function of deviation, dispersion, and number of measurements. This criterion was used in this study as the selection system of the input data set¹. The standard deviation was first determined and a dispersion of ± 3 standard deviations was found to be the bound of the input data

1. The "Chauvenet's Criterion of Rejection" was first designed and programmed by P. McGrath, University of Manitoba.

set. The data values which exceed the boundary limits will then be cut down to the appropriate boundary values. This not only served the purpose of removing unwanted spikes, it also removed the anomalous peaks which might result from local iron formation.

Additional rows and columns of numeric zeros were added to the data matrix during the data preparation stage in order to satisfy the prime factor assumption of the fast Fourier transform algorithm (see Section 2.4). The presence of these zeros in the data matrix introduced a step-like function at the boundaries and severe edge effects resulted if they were not eliminated. This search and elimination process was also introduced into the screening system of this project. This was done by means of replacing numeric zeros found in the input matrix by the average value (or mean) of the data set.

If the data have a regional trend, spurious components at all frequencies will be introduced in the Fourier Transform. Best-fit plane produced by a least-squares fit has been commonly used for regional trend extraction. The plane was subtracted from the data set to produce a new set of data with zero regional trend. This approach was not used in the present study. Instead, a numerical model of the sufficient complexity, including adequate secular variation correction was used as a suitable representation of the

regional field. This is the best known and most widely used field model: the International Geomagnetic Reference Field (IGRF). The IGRF values were computed at every grid point of the data matrix by means of a computer program² and it was subtracted from the field value at that grid point. This removes the regional trend from the data before the filtering process. A more detailed account of the IGRF surface can be found in Section 2.5.

2.4 The Fast Fourier Transform

The Fourier transform has long been a principle analytical tool in such diverse fields as linear systems, optics and signal analysis. The advent of the development of the fast Fourier Transform (FFT), an algorithm that efficiently computes the discrete Fourier transform which reduces the enormous amount of computation time adds even more applications to this powerful analytical technique. The fast Fourier transform algorithm was the principal tool used in this thesis to study the potential field data.

The potential field data $f(x,y)$ is considered as a mixture of random noise and aperiodic signals. The spectral

2. Computer program supplied by the Institute of Geological Sciences, Hailsham.

decomposition of the potential field data $f(x,y)$ can be represented by the following complex Fourier transform relations in the digital domain.

$$F(K_1, K_2) = \sum_{x=0}^{N-1} \sum_{y=0}^{N-1} f(x,y) e^{\frac{2\pi i}{N}(K_1 x + K_2 y)}$$

$$\text{for } K_1, K_2 = 0, 1, 2, \dots (N-1)$$

and conversely

$$f(x,y) = \frac{1}{N^2} \sum_{K_1=0}^{N-1} \sum_{K_2=0}^{N-1} F(K_1, K_2) e^{-\frac{2\pi i}{N}(K_1 x + K_2 y)}$$

$$\text{for } x, y = 0, 1, 2, \dots (N-1)$$

where $F(K_1, K_2)$ are N complex-valued vectors. The wavelengths λ_1 and λ_2 are given by $\frac{2\pi}{K_1}$ and $\frac{2\pi}{K_2}$, where K_1 and K_2 are the wave-numbers along the x and y directions.

The fast Fourier transform was developed from these fundamental equations. The criteria for the formulation of these equations and their various properties have been dealt with thoroughly by Good (1958), Cooley and Tukey (1965) and Gentleman and Sande (1966). In general, direct computations of the Fourier transform require N^2 operations, where N is the size of the input vector. Fast Fourier transform (FFT) algorithm offers a much faster route of less than $KN \log_K N$ operations (K is a factor of N). In other words,

one can obtain the transforms $(\frac{N^2}{KN \log_K N})$ times faster. The accuracy of the results is also increased by the same ratio.

The fundamental basis of the fast Fourier transform algorithm is to decompose each data vector into simple factors. (For example, $N = K_1 \cdot K_2 \cdot K_3 \cdot \dots \cdot K_n$). Then, the elementary transformations were followed by a permutation sorting procedure to produce the required coefficients. In the same manner, a two-dimensional data set such as the aeromagnetic field data in this project can be considered as a vector (size N_1 by N_2) of length $N = N_1 N_2$ which the fast Fourier algorithm can be applied in the usual way.

2.5 Background Field Analysis

The earth's total magnetic field is composed of the field generated by the earth's core plus anomalous fields which are attributed to the magnetic properties of shallow and deep crustal sources. An important application of aeromagnetic surveys is to interpret the magnetic properties or characteristics of deep crustal magnetic sources. These deep magnetic sources generate long wavelength anomalies which are often low in amplitude, usually less than 200 nanotesla. As a result, the core generated background field plays an important role in the interpretation of the long-wavelength aeromagnetic anomalies. This core generated field